Quantum entanglement and quantum phase transition in the XY model with staggered Dzyaloshinskii-Moriya interaction

Fu-Wu Ma, Sheng-Xin Liu, and Xiang-Mu Kong

Phys. Rev. A **84**, 042302 — Published 3 October 2011

DOI: 10.1103/PhysRevA.84.042302

Quantum entanglement and quantum phase transition in the XY model with staggered Dzyaloshinskii-Moriya interaction

Fu-Wu Ma, Sheng-Xin Liu and Xiang-Mu Kong*

Shandong Provincial Key Laboratory of Laser Polarization and Information Technology, Department of Physics, Qufu Normal University, Qufu 273165, China

Abstract

We study the quantum entanglement and quantum phase transition (QPT) of the anisotropic spin-1/2 XY model with staggered Dzyaloshinskii-Moriya (DM) interaction by means of quantum renormalization group method. The scaling of coupling constants and the critical points of the system are obtained. It is found that when the number of renormalization group iterations tends to infinity, the system exhibit a QPT between the spin-fluid and Néel phases which correspond with two saturated values of the concurrence for a given value of the strength of DM interaction. The DM interaction can enhance the entanglement and influence the QPT of the system. To gain further insight, the first derivative of the entanglement exhibit a nonanalytic behavior at the critical point and it directly associates with the divergence of the correlation length. This shows that the correlation length exponent is closely related to the critical exponent, i.e., the scaling behaviors of the system.

PACS numbers: 03.67.Mn, 73.43.Nq, 75.10.Pq, 64.60.ae

*Corresponding author; Electronic address: kongxm@mail.qfnu.edu.cn

I. INTRODUCTION

In the quantum systems, entanglement is a pure quantum correlation, which is the fundamental difference between quantum and classical physics [1]. In recent years, quantum entanglement has attracted much attention in quantum information theory because of its importance in developing the idea of quantum computers and other quantum information devices [2, 3]. It has also been realized as a crucial resource to process and send information in different ways, such as quantum teleportation, quantum cryptography, and algorithms for quantum computations [4–6]. In the condensed-matter physics, it is very significant to discuss the relation between entanglement and quantum phase transition (QPT) which has been attracted many researchers to investigate [7–9].

For discussing the properties of many-body systems, the renormalization-group (RG) method is applied. In the past several decades, much effort had been investigated in many spin systems using this method. Real space renormalization group method was applied to discuss the critical points and phase diagrams of Heisenberg and Blume-Capel models [10–13]. These properties of many models were also studied by Monte Carlo RG [14, 15]. The density-matrix RG method which is a powerful numerical method is used to study the ground and low-lying states properties of low-dimensional lattice models. It has been applied successfully to lots of strongly correlated systems in 1D as well as 2D systems [16–19]. In the finite temperature, many physical quantities, such as the energy spectrum, the magnetic moment, magnetic susceptibility, fidelity susceptibility and the thermal entanglement, are discussed by Jordan-Wigner transformation [20–23]. Recently, the pairwise entanglement of the system is studied by the quantum renormalization-group (QGR) method which plays an important role in QPT [24, 25]. The spin-1/2 Ising and Heisenberg models were investigated by the same method and it is found that the systems exist QPT and nonanalytic behavior, such as the discontinuity in the quantum critical points [26–29]. For getting the accurate results, the XXZ model with next-nearest-neighbor interactions are investigated [30, 31]. It is found that the tri-critical point and the phase diagram of the system can be obtained. We have studied the XY model by using the same method, and find that the system exhibits a QPT [32].

Some spin models can be supplemented with a magnetic term which is called Dzyaloshinskii-Moriya (DM) interaction arising from the spin-orbit coupling. The DM in-

teraction, which was proposed by Dzyaloshinskii and Moriya about half century ago [33, 34], can influence the phase transition and the critical properties of many systems. The relevance of antisymmetric superexchange interaction which describes quantum antiferromagnetic system was introduced by Dzyaloshinskii. Moriya found that such interaction arises naturally in the perturbation theory in magnetic systems with low symmetry. Recently, Ising and XXZ models with DM interaction, the form of which for two spins $\overrightarrow{S_i}$ and $\overrightarrow{S_j}$ is $\overrightarrow{D} \cdot \left(\overrightarrow{S_i} \times \overrightarrow{S_j}\right)$, were studied in Ref. [26, 27]. It is found that the critical points of the systems divide the systems into two phases, i.e., spin-fluid and Néel phases. The nonanalytic behavior of the first derivative of the entanglement and the scaling behavior of the systems are also gotten at the critical point. The staggered DM interaction is also important for discussing the ferromagnetism, which was investigated in the Ref. [35].

The quantum entanglement and QPT of the spin-1/2 XY model with staggered DM interaction are discussed by using QRG method. We obtain the stable and unstable fixed points of the system. It is found that the phase transition point is changed as the DM interaction increases. The concurrence is calculated which is influenced by the anisotropy parameter and DM interaction. The concurrence tends to two fixed values which associate with the phases of the system as the number of RG iteration increases. Furthermore, the first derivative of the concurrence shows nonanalytic behavior at the critical point which has relation with the correlation length.

This paper is organized as follows. In Sec. II, we apply QRG method to investigate the model and obtain the fixed points. In Sec. III, the entanglement between two blocks is investigated, and we further discuss the nonanalytic and the scaling behaviors of the entanglement. We summarize in Sec. IV.

II. QUANTUM RENORMALIZATION GROUP OF THE MODEL

The mode elimination or the thinning of the degrees of freedom followed by an iteration, which reduces the number of lattices step by step until reaching a more tractable circumstance, is the main idea of RG method. RG is a proper method to give the universal behavior at long wavelengths, it includes many methods, such as decimation, bond-moving and cumulant expansion. In this paper, the Kadanoff's block approach is implemented where we have consider three sites as a block (marking as 1-2-3). Generally speaking, this method

contains three steps. Firstly, the system is divided into blocks and the Hamiltonian of each block can be exactly diagonalized and solved. Then, the projection operator is builded by the lower eigenvectors. And finally, the full Hamiltonian is projected onto these eigenvectors to obtain the effective Hamiltonian which acts on the renormalized subspace, i.e., the RG equations [36, 37].

The Hamiltonian of 1D anisotropic XY model with staggered DM interaction on a periodic chain of N sites can be written as

$$H_0 = \frac{J}{4}\sum_{i=1}^{N}\left[(1+\gamma)\,\sigma_i^x\sigma_{i+1}^x + (1-\gamma)\,\sigma_i^y\sigma_{i+1}^y + (-1)^i\,D\left(\sigma_i^x\sigma_{i+1}^y - \sigma_i^y\sigma_{i+1}^x\right)\right], \tag{1}$$

where J is the nearest exchange coupling constant, γ is the anisotropy parameter, D is the strength of DM interaction in the direction of z, and σ_i^α ($\alpha = x, y$) are Pauli operators of the ith site. For the above model, when $\gamma = D = 0$, the model becomes isotropic XX model; when $\gamma = 1$ and $D = 0$, it turns into the Ising model which was exactly solved in Ref. [38].

The initial Hamiltonian H_0 acts on the effective Hilbert space and then the effective Hamiltonian H^{eff} can be gotten. The essential criterion for RG is that H^{eff} have similar structure to H_0, but we can not get this, i.e., the signs of $\sigma_i^y\sigma_{i+1}^y$ and $\sigma_i^y\sigma_{i+1}^x$ terms are changed. To avoid this and produce a self-similar Hamiltonian, we implement a π rotation around the x axis for all even sites and leave all odd sites unchanged [29]. Therefore, the transformed Hamiltonian is obtained as follows,

$$H = \frac{J}{4}\sum_{i=1}^{N}\left[(1+\gamma)\,\sigma_i^x\sigma_{i+1}^x - (1-\gamma)\,\sigma_i^y\sigma_{i+1}^y + D\left(\sigma_i^x\sigma_{i+1}^y + \sigma_i^y\sigma_{i+1}^x\right)\right]. \tag{2}$$

We discuss our final results in terms of above Hamiltonian.

For the Kadanoff's block approach, H can be written as

$$H = H^B + H^{BB}, \tag{3}$$

where H^B is the block Hamiltonian and H^{BB} is the interblock Hamiltonian. The explicit forms of H^B and H^{BB} are

$$H^B = \sum_{l=1}^{N/3} h_l^B, \tag{4}$$

$$H^{BB} = \frac{J}{4}\sum_{l=1}^{N/3}\left[(1+\gamma)\,\sigma_{l,3}^x\sigma_{l+1,1}^x - (1-\gamma)\,\sigma_{l,3}^y\sigma_{l+1,1}^y + D\left(\sigma_{l,3}^x\sigma_{l+1,1}^y + \sigma_{l,3}^y\sigma_{l+1,1}^x\right)\right], \tag{5}$$

where the lth block Hamiltonian is

$$h_l^B = \frac{J}{4}\left[(1+\gamma)\left(\sigma_{l,1}^x\sigma_{l,2}^x + \sigma_{l,2}^x\sigma_{l,3}^x\right) - (1-\gamma)\left(\sigma_{l,1}^y\sigma_{l,2}^y + \sigma_{l,2}^y\sigma_{l,3}^y\right)\right.$$
$$\left. + D\left(\sigma_{l,1}^x\sigma_{l,2}^y + \sigma_{l,1}^y\sigma_{l,2}^x + \sigma_{l,2}^x\sigma_{l,3}^y + \sigma_{l,2}^y\sigma_{l,3}^x\right)\right]. \tag{6}$$

In terms of matrix product states [39], we can get the eigenvalues and eigenvectors by exactly solving h_l^B. The ground states which are doubly-degeneracy are useful to construct the projection operator and calculate the entanglement in later. In the standard basis $\{|\uparrow\uparrow\uparrow\rangle, |\uparrow\uparrow\downarrow\rangle, |\uparrow\downarrow\uparrow\rangle, |\uparrow\downarrow\downarrow\rangle, |\downarrow\uparrow\uparrow\rangle, |\downarrow\uparrow\downarrow\rangle, |\downarrow\downarrow\uparrow\rangle, |\downarrow\downarrow\downarrow\rangle\}$, the degenerate ground states are given by

$$|\varphi_0\rangle = \frac{\sqrt{1+D^2}}{\sqrt{2}q}\left[\frac{-q}{\sqrt{2}\,(Di+1)}|\uparrow\uparrow\downarrow\rangle + \frac{\gamma}{Di+1}|\uparrow\downarrow\uparrow\rangle + \frac{-q}{\sqrt{2}\,(Di+1)}|\downarrow\uparrow\uparrow\rangle + |\downarrow\downarrow\downarrow\rangle\right], \tag{7}$$

$$|\varphi_0\rangle' = \frac{1}{2}\left[\frac{-\sqrt{2}\,(1-Di)}{q}|\uparrow\uparrow\uparrow\rangle + |\uparrow\downarrow\downarrow\rangle + \frac{-\sqrt{2}\gamma}{q}|\downarrow\uparrow\downarrow\rangle + |\downarrow\downarrow\uparrow\rangle\right], \tag{8}$$

where $q = \sqrt{1+D^2+\gamma^2}$, $|\uparrow\rangle$ and $|\downarrow\rangle$ are the basis vectors of σ^z in itself representation. The energy corresponding to the ground states is

$$e_0 = -q/\sqrt{2}.$$

We keep the ground states of h_l^B to define the effective site. The effective Hamiltonian H^{eff} and the Hamiltonian H have in common the low lying spectrum [40]. An exactly implementation of this is given by the following equation,

$$H^{\text{eff}} = T^\dagger H T. \tag{9}$$

In the preceding equation, $T = \prod_{l=1}^{N/3} T_0^l$ is the projection operator of the system and the specific form of T_0^l is

$$T_0^l = |\Uparrow\rangle_l \langle\varphi_0| + |\Downarrow\rangle_l \langle\varphi_0|', \tag{10}$$

where $|\Uparrow\rangle_l$ and $|\Downarrow\rangle_l$ are the renamed states of each block in the effective space, which can be seen as a different spin-1/2 particle. Here, we consider only the first-order correction in the perturbation theory. By using the Eq. (3), the Eq. (9) can be written as

$$H^{\text{eff}} = T^\dagger\left(H^B + H^{BB}\right)T = T^\dagger H^B T + T^\dagger H^{BB} T, \tag{11}$$

The Pauli matrices in x and y directions of renormalization are obtained as follows,

$$\begin{aligned} T_0^{l\dagger}\sigma_{l,j}^x T_0^l &= \xi_j \sigma_l^{'x} + \zeta_j \sigma_l^{'y}, \\ T_0^{l\dagger}\sigma_{l,j}^y T_0^l &= \mu_j \sigma_l^{'x} + \nu_j \sigma_l^{'y} \quad (j=1,2,3)\,, \end{aligned} \tag{12}$$

where

$$\begin{aligned} \xi_1 = \xi_3 &= \frac{1+D^2+\gamma}{\sqrt{2\left(1+D^2\right)}q},\ \zeta_1 = \zeta_3 = \frac{-\gamma D}{\sqrt{2\left(1+D^2\right)}q}, \\ \xi_2 &= -\frac{1}{2\sqrt{1+D^2}} - \frac{\sqrt{1+D^2}\gamma}{q^2},\ \zeta_2 = \frac{D}{2\sqrt{1+D^2}}, \\ \mu_1 = \mu_3 &= \frac{\gamma D}{\sqrt{2\left(1+D^2\right)}q},\ \nu_1 = \nu_3 = \frac{\gamma - 1 - D^2}{\sqrt{2\left(1+D^2\right)}q}, \\ \mu_2 &= -\frac{D}{2\sqrt{1+D^2}},\ \nu_2 = -\frac{1}{2\sqrt{1+D^2}} + \frac{\sqrt{1+D^2}\gamma}{q^2}. \end{aligned} \tag{13}$$

We substitute them into Eq. (11) and obtain the effective Hamiltonian,

$$H^{\text{eff}} = \frac{J^{'}}{4}\sum_{k=1}^{N/3}\left[\left(1+\gamma^{'}\right)\sigma_k^x\sigma_{k+1}^x - \left(1-\gamma^{'}\right)\sigma_k^y\sigma_{k+1}^y + D^{'}\left(\sigma_k^x\sigma_{k+1}^y + \sigma_k^y\sigma_{k+1}^x\right)\right], \tag{14}$$

where

$$J^{'} = \frac{1+D^2+3\gamma^2}{2q^2}J,\ \gamma^{'} = \frac{3\gamma+3D^2\gamma+\gamma^3}{1+D^2+3\gamma^2},\ D^{'} = -D. \tag{15}$$

Because the antisymmetric is the special property of DM interaction, i.e., $\overrightarrow{D}_{i,j} = -\overrightarrow{D}_{j,i}$, the stable and unstable fixed points can be gotten by only solving $\gamma^{'} \equiv \gamma$. The stable fixed points locate at $\gamma = \pm\sqrt{1+D^2}$ and $\gamma = \infty$, the unstable fixed point is $\gamma = 0$ which separates the spin-fluid phase, $\gamma = 0$ and $\gamma = \infty$, from the Néel phase, $0 < |\gamma| < \sqrt{1+D^2}$.

III. RENORMALIZATION ENTANGLEMENT ANALYSIS

There are many measures for pairwise entanglement [41–44]. In this section, we would like to calculate the concurrence of pure state where we consider one of the degeneracy ground states. The density matrix of a ground state is composed, i.e.,

$$\rho = |\varphi_0\rangle\langle\varphi_0|\,. \tag{16}$$

The results of using $\left|\varphi_0^{'}\right\rangle$ to construct the density matrix will be same as Eq. (16).

There are two cases to define the concurrence for a three-site block. (i) The concurrence between sites 1 and 3 is obtained by summing over the degrees of freedom of the middle site 2. (ii) We trace over the site 1 or 3 and get the concurrence between the middle site 2 and the other one. Without loss of generality, we consider the case (i). In the standard basis $\{|\uparrow\uparrow\rangle, |\uparrow\downarrow\rangle, |\downarrow\uparrow\rangle, |\downarrow\downarrow\rangle\}$, the reduced density matrix ρ_{13} for sites 1 and 3 can be gotten in Eq. (16),

$$\rho_{13} = \mathrm{Tr}_2[\rho] = \frac{1+D^2}{2q^2}\begin{pmatrix} \frac{\gamma^2}{1+D^2} & 0 & 0 & \frac{i\gamma}{D+i} \\ 0 & \frac{q^2}{2(1+D^2)} & \frac{q^2}{2(1+D^2)} & 0 \\ 0 & \frac{q^2}{2(1+D^2)} & \frac{q^2}{2(1+D^2)} & 0 \\ \frac{-i\gamma}{D-i} & 0 & 0 & 1 \end{pmatrix}. \tag{17}$$

C_{13} denotes the concurrence between the sites 1 and 3, which is defined as

$$C_{13} = \max\{\lambda_1 - \lambda_2 - \lambda_3 - \lambda_4,\ 0\}, \tag{18}$$

where λ_k $(k = 1, 2, 3, 4)$ are the square roots of eigenvalues of $R = \rho_{13}\tilde{\rho}_{13}$ in descending order. $\tilde{\rho}_{13}$ is the spin-flipped state [44] and its definition is

$$\tilde{\rho}_{13} = (\sigma_1^y \otimes \sigma_3^y)\, \rho_{13}^*\, (\sigma_1^y \otimes \sigma_3^y), \tag{19}$$

where ρ_{13}^* is the complex conjugate of ρ_{13}. The value of C_{13} ranges from 0 to 1, if $C_{13} = 0$ or 1, the system is in an unentangled or a maximally entangled state, else it corresponds to a partial entangled state. The square eigenvalues of R are gotten,

$$\lambda_1 = \frac{1}{2},\ \lambda_2 = \frac{\gamma\sqrt{1+D^2}}{q},\ \lambda_3 = \lambda_4 = 0. \tag{20}$$

Thus, the concurrence is obtained as follows,

$$C_{13} = \max\{\lambda_1 - \lambda_2,\ 0\} = \frac{1}{2} - \frac{\gamma\sqrt{1+D^2}}{q}. \tag{21}$$

It is easy to see that C_{13} is influenced by γ and D. For three-site model, we plot C_{13} versus γ for different values of D in Fig. 1. From the figure, it is found that the entanglement is a fixed value regardless of any value of D at $\gamma = 0$ or infinity. That is to say there are not phase transition for the XX model. Moreover, the DM interaction which enhances the entanglement of the system plays an important role when γ is small comparing to D, while the effect of anisotropy parameter for the entanglement is more important than DM interaction when γ is large.

The purpose of QRG is that the full properties of the model enter a few sites through the renormalizing of coupling constants. The renormalization of the strength of DM interaction and anisotropic parameter are obtained which are contribution to the concurrence of the system. For a fixed value of $D = 1$, the graph for C_{13} and γ is plotted in Fig. 2. It reveals that as the number of QRG iterations increases, the concurrence develops three rather different features which are separated by $\gamma = 0$ and $\gamma = \sqrt{2}$. When the number of RG iterations is very large, i.e., the system is infinity, the value of C_{13} is zero corresponding to Néel phase for γ ranging from $-\sqrt{2}$ to $\sqrt{2}$ except the point of 0; at $\gamma = 0$, the system is the spin-fluid phase corresponding to the maximum value of the concurrence; for $|\gamma| > \sqrt{2}$, the concurrence of the system slowly increases with $|\gamma|$ increasing and finally reaches to the maximum value. The system is in the same phase for $\gamma = 0$ and $\gamma = \infty$. For this, it can be explained from the Hamiltonian, i.e., the anisotropic XY model changes the isotropic XX model for $\gamma = 0$ and $\gamma = \infty$.

Further insight, when the system is large enough, the first derivation of the entanglement shows the nonanalytic behavior at the critical point. Because $dC_{13}/d\gamma$ is an even function of γ, we have only plotted $dC_{13}/d\gamma$ in $\gamma \geq 0$ for $D = 1$ in Fig. 3. When the QRG iteration trends infinity, there are a minimum and a maximum values for each plot. From the diagram, it is found that the singular behavior of the concurrence becomes more pronounced at the thermodynamic limit. This indicates that the system exhibit a QPT which is a second-order QPT. For the inset of diagram, there is a maximum value for each curved shape which verges to zero as the system becomes large. These also manifest that there are same properties for $\gamma = 0$ and $\gamma = \infty$. For a more detailed analysis, the positions of the minimum or the maximum of $dC_{13}/d\gamma$ with the size of system increasing are given in Fig. 4. It can be seen that it shows a linear behavior, i.e. the scaling behavior of the system. The critical exponent θ for this behavior is $dC_{13}/d\gamma|_{\gamma_{\min}}$ or $dC_{13}/d\gamma|_{\gamma_{\max}} \sim N^{0.98}$. These results justify that θ is the reciprocal of the correlation length exponent υ closing to the critical point, i.e., $\theta = 1/\upsilon$.

Similarly, we also investigate how the concurrence versus D changes for a fixed value of γ. The concurrence with D changing for different iterations is depicted in Fig. 5. It is clearly seen that the concurrence becomes large with D increasing and then until to 0.5 at last. But the larger the size of system is, the slower the increasing tendency of the concurrence is. It is implied that the system can not occur QPT by changing the DM interaction. The first partial derivative of concurrence for D is clearly discussed in Fig. 6. There is not suddenly

mutative in the diagram, but the maximum value of each plot becomes small with the size of the system largening. While we can also get the linear behavior between the maximum of dC_{13}/dD and the corresponding size of system which is plotted in Fig. 7. The exponent for the curve is $dC_{13}/dD|_{D_{\max}} \sim N^{-0.98}$. It falls into the Ising-like universality class. The position of the maximum of concurrence tends to infinity as the iteration of QRG increases, in other words, the stable fixed point $D \to \infty$ is reached.

IV. CONCLUSIONS

The relation between the concurrence as a measure of quantum correlations and QPT was discussed. The anisotropy and DM interaction parameters determined the phase diagrams of the model. If the anisotropy parameter was small, the concurrence depended on the DM interaction, else the anisotropy parameter played an important role. As the number of RG iterations increased, the concurrence developed two different values which separated two phases for a given D, i.e., spin-fluid phase and Néel phase. For Néel phase, the larger the value of D was, the wider the width of value of γ was. The critical behavior was described by the first derivative of the concurrence of the blocks. The scaling behavior characterizes how the critical point of the model was touched as the size of system increased. The critical exponent had relation with the correlation length exponent in the vicinity of the critical point. It is shown that the quantum critical properties of the model were closely associated with the behavior of the entanglement. The concurrence increased slowly as the the size of the system became large, but the tendency of concurrence was unanimous, namely trending a fixed value.

Acknowledgments

This work is supported by the National Natural Science Foundation of China under Grant No. 10775088, the Shandong Natural Science Foundation under Grant No. ZR2011AM018, and the Specialized Research Fund for the Doctoral Program of Higher Education under Grant No. 20103705110001. Fu-Wu Ma would like to thank Yin-Yang Shen, Sha-Sha Li and

Hong Li for many fruitful discussions and useful comments.

---

[1] C. H. Bennett, G. Brassard, C. Crepeau, R. Jozsa, A. Peres, and W. K. Wootters, Phys. Rev. Lett. 70, 1895 (1993).

[2] S. B. Zheng and G. C. Guo, Phys. Rev. Lett. 85, 2392 (2000).

[3] M. A. Nielsen and I. L. Chuang, *Quantum Computation and Quantum Communication* (Cambridge University Press, Cambridge, England, 2000).

[4] C. H. Bennett, G. Brassard, C. Crepeau, R. Jozsa, A. Peres, and W. K. Wootters, Phys. Rev. Lett. 70, 1895 (1993).

[5] A. K. Ekert, Phys. Rev. Lett. 67, 661 (1991).

[6] D. Deutsch and R. Jozsa, Proc. R. Soc. London, Ser. A 439, 553 (1992).

[7] A. Osterloh, L. Amico, G. Falci, and R. Fazio, Nature (London) 416, 608 (2002).

[8] S. Sachdev, *Quantum Phase Transitions* (Cambridge University Press, Cambridge, 2000).

[9] T. J. Osborne and M. A. Nielsen, Phys. Rev. A 66, 032110 (2002).

[10] Z. Friedman, Phys. Rev. Lett. 36, 1326 (1976).

[11] R. C. Brower, F. Kuttner, M. Nauenberg, and K. Subbarao, Phys. Rev. Lett. 38, 1231 (1977).

[12] A. L. Stella and F. Toigo, Phys. Rev. B 17, 2343 (1978).

[13] N. B. Branco, Phys. Rev. B 56, 11673 (1997).

[14] S. K. Ma, Phys. Rev. Lett. 37, 461 (1976).

[15] P. J. Reynolds, H. E. Stanley, and W. Klein, Phys. Rev. B 21, 1223 (1980).

[16] S. R. White, Phys. Rev. Lett. 69, 2863 (1992); Phys. Rev. B 48, 10345 (1993).

[17] T. Xiang, Phys. Rev. B 53, 10445 (1996).

[18] T. Nishino, J. Phys. Soc. Jpn. 64, 3598 (1995).

[19] S. R. White and D. J. Scalapino, Phys. Rev. Lett. 80, 1272 (1998).

[20] C. D. Batista and G. Ortiz, Phys. Rev. Lett. 86, 1082 (2001).

[21] T. J. osborne and M. A. Nielsen, Phys. Rev. A 66, 032110 (2002).

[22] L. A. Wu, M. S. Sarandy, D. A. Lidar, and L. J. Sham, Phys. Rev. A 74, 052335 (2006).

[23] Y. C. Li and S. S Li, Phys. Rev. A 79, 032338 (2009).

[24] P. Pefeuty, R. Jullian, and K. L. Penson, *in Real-Space Renormalizaton*, edited by T. W. Burkhardt and J. M. J. van Leeuwen (Springer, Berlin, 1982), Chap. 5.

[25] K. G. Wilson, Rev. Mod. Phys. 47, 773 (1975).

[26] R. Jafari, M. Kargarian, A. Langari, and M. Siahatgar, Phys. Rev. B 78, 214414 (2008).

[27] M. Kargarian, R. Jafari, and A. Langari, Phys. Rev. A 79, 042319 (2009).

[28] M. Kargarian, R. Jafari, and A. Langari, Phys. Rev. A 77, 032346 (2008); 76, 060304 (2007).

[29] A. Langari, Phys. Rev. B 69, 100402 (R) (2004).

[30] R. Jafari and A. Langari, Phys. A, 364, 213 (2006).

[31] R. Jafari and A. Langari, Phys. Rev. B, 76, 014412 (2007).

[32] F. W. Ma, S. X. Liu, and X. M. Kong, Phys. Rev. A 83, 062309, (2011).

[33] I. Dzyaloshinsky, J. phys Chem. Solids 4, 241 (1958).

[34] T. Moriya, Phys. Rev. 120, 91 (1960).

[35] J. H. H. Perk and H. W. Capel, Phys. Lett. A, 58 115 (1976).

[36] M. A. Martín-Delgado and G. Sierra, Int. J. Mod. Phys. A 11, 3145 (1996).

[37] A. Langari, Phys. Rev. B 58, 14467 (1998).

[38] Th. M. Nieuwenhuizen and J. M. Luck, J. Phys. A: Math. Gen 19, 1207 (1986).

[39] F. Verstraete, J. I. Cirac, J. I. Latorre, E. Rico, and M. M. Wolf, Phys. Rev. Lett. 94, 140601 (2005).

[40] José González, Miguel A. MartÍn-Deigado, Germán Sierrra, Angeles H. Vozmediano, *Quantum Electron Liquids and high-T_c Superconductivity*, edited by W. Beiglböck (Springer, Berlin 1995), Chap. 11.

[41] Y. X. Chen and D. Yang, Quantum Information Processing. 1, 389 (2003).

[42] G. Vidal and R. F. Werner, Phys. Rev. A 65, 032314 (2002).

[43] E. M. Rains, Phys. Rev. A 60, 179 (1999).

[44] S. Hill and W. K. Wootters, Phys. Rev. Lett. 78, 5022 (1997); W. K. Wootters, Phys. Rev. Lett. 80, 2245 (1998).

Figure captions

Fig 1. (Color online) Concurrence between the first and third sites of a three-site model in terms of anisotropy for different values of the strength of DM interaction.

Fig 2. (Color online) Representation of the evolution of the concurrence in terms of QRG iterations at a fixed value of $D = 1$. The inset of diagram of γ ranges from $-\sqrt{2}$ to $\sqrt{2}$.

Fig 3. (Color online) First derivative of concurrence and its manifestation toward diverging as the number of QRG iterations increases (Fig. 2). The value of the inset of diagram manifestation toward zero.

Fig 4. (Color online) The logarithm of the absolute value of minimum or maximum, $\ln(|dC_{13}/d\gamma|\gamma_m|)$, versus the logarithm of chain size, $\ln(N)$, which shows a scaling behavior. Each point corresponds to the minimum or maximum value of a single plot of Fig. 3. (a) γ ranges from 0 to $\sqrt{2}$, (b) γ is bigger than $\sqrt{2}$.

Fig 5. (Color online) Representation of the evolution of the concurrence in terms of QRG iterations at a fixed value of $\gamma = \sqrt{2}$.

Fig 6. (Color online) First derivative of concurrence and its manifestation toward zero as the number of QRG iterations increases (Fig. 5).

Fig 7. (Color online) The logarithm of the absolute value of maximum, $\ln(|dC_{13}/dD|D_{\max}|)$, versus the logarithm of chain size, $\ln(N)$, which is linear and shows a scaling behavior. Each point corresponds to the maximum value of a single plot of Fig. 6.

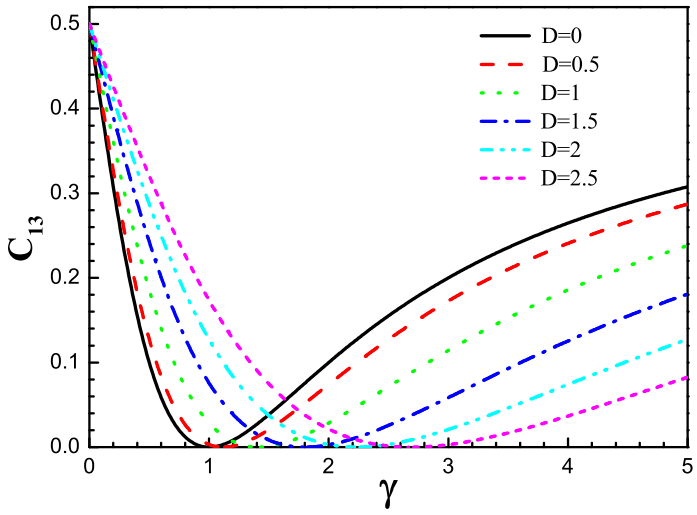

Figure 1 AG10793 06Sep2011

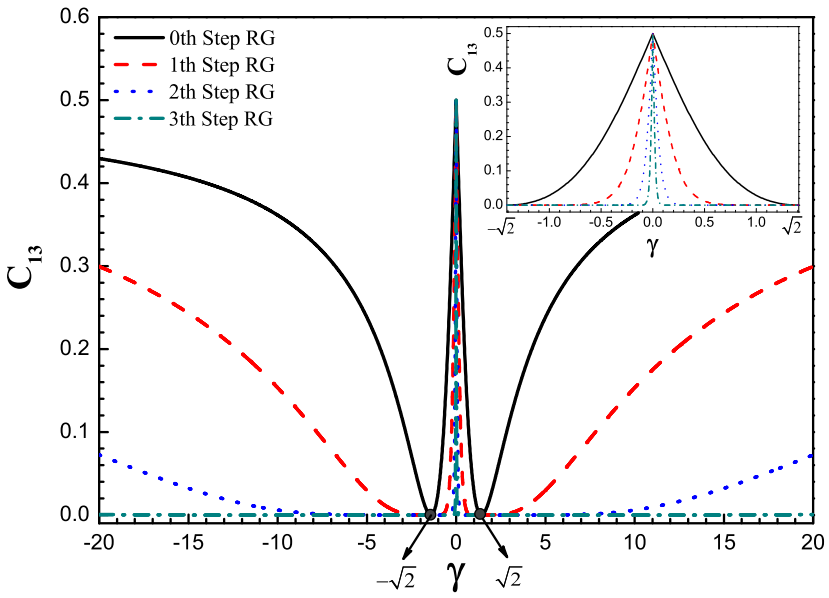

Figure 2 AG10793 06Sep2011

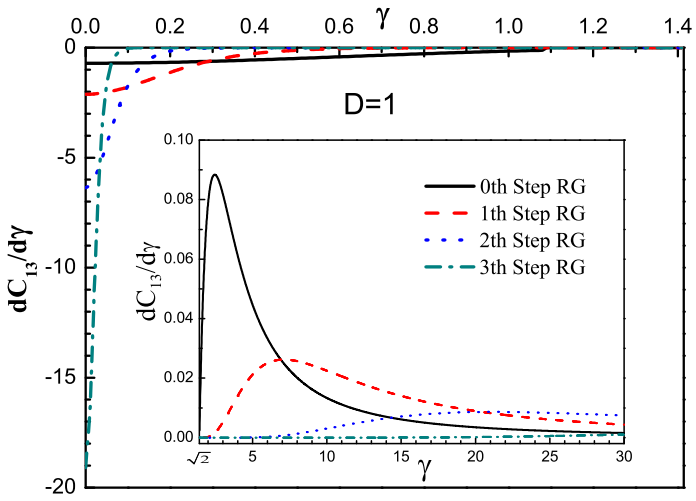

Figure 3 AG10793 06Sep2011

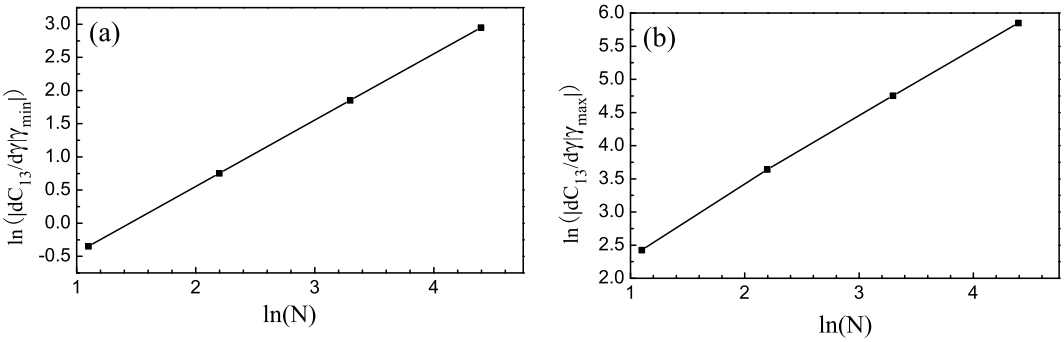

Figure 4 AG10793 06Sep2011

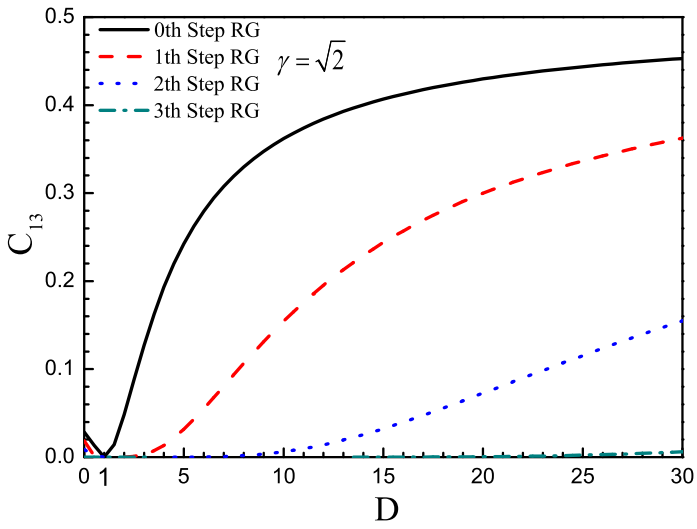

Figure 5 AG10793 06Sep2011

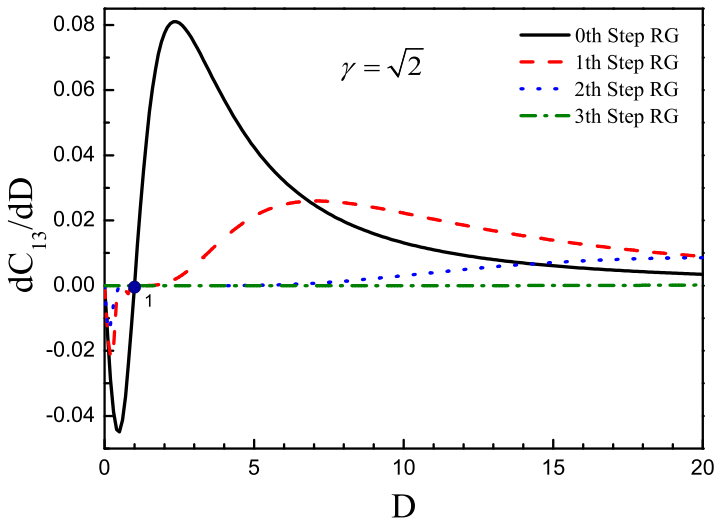

Figure 6 AG10793 06Sep2011

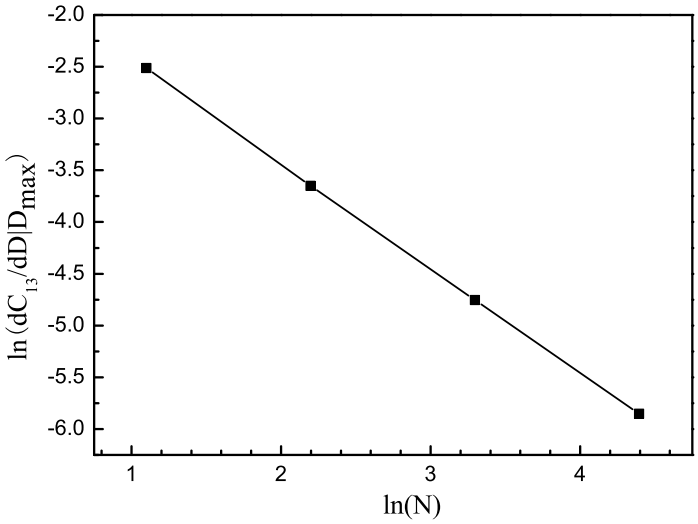

Figure 7 AG10793 06Sep2011